UNITED STATES
DEPARTMENT OF THE INTERIOR
GEOLOGICAL SURVEY

LABORATORY INVESTIGATIONS OF THE PHYSICS OF STEAM FLOW IN A POROUS MEDIUM

By W.N. Herkelrath and A.F. Moench

Open-File Report 82-95
Menlo Park, California
January, 1982

CONTENTS

TABLES

ILLUSTRATIONS

LABORATORY INVESTIGATIONS OF THE PHYSICS OF STEAM FLOW IN A POROUS MEDIUM

-

by W.N. Herkelrath and A.F. Moench

-

ABSTRACT

Experiments were carried out in the laboratory to test a theory of transient flow of pure steam in a uniform porous medium. This theory is used extensively in modeling pressure-transient behavior in vapor-dominated geothermal systems. Transient, superheated steam-flow experiments were run by bringing a cylinder of porous material to a uniform initial pressure, and then making a step increase in pressure at one end of the sample, while monitoring the pressure-transient breakthrough at the other end. It was found in experiments run at 100°, 125°, and 146°C that the time required for steam-pressure transients to propagate through an unconsolidated material containing sand, silt, and clay was 10 to 25 times longer than predicted by theory. It is hypothesized that the delay in the steam-pressure transient was caused by adsorption of steam in the porous sample.

In order to account for steam adsorption, a sink term was included in the conservation of mass equation. In addition, energy transfer in the system has to be considered because latent heat is released when steam adsorption occurs, increasing the sample temperature by as much as 10°C. Finally, it was recognized that the steam pressure was a function of both the temperature and the amount of adsorption in the sample. For simplicity, this function was assumed to be in equilibrium adsorption isotherm, which was determined by experiment. By solving the modified mass and energy equations numerically,

subject to the empirical adsorption isotherm relationship, excellent theoretical simulation of the experiments was achieved.

The experiments support the hypothesis that adsorption of steam can strongly influence steam pressure-transient behavior in porous media; the results suggest that the modified steam-flow theory, which includes steam adsorption terms, should be used in modeling steam flow in vapor-dominated geothermal systems.

INTRODUCTION

Quantitative understanding of the physics of the flow of steam in porous media is important in modeling of fluid transport in geothermal systems, high-level nuclear waste repositories, and heat-storage aquifers. Numerical modeling efforts in these research areas are supported by laboratory experiments and verified with field tests. The primary role of laboratory work is to test the fundamental equations that are being used in the models. Modeling of high-temperature fluid transport generally involves extrapolation of existing theories to temperature and pressure regimes in which equations have not been tested in controlled laboratory investigations. Laboratory experiments also provide test cases for computer simulation. This is important because generally there is no analytical solution to check numerical solutions of model equations, that are often highly nonlinear in the case of the simultaneous transport of mass and energy. In this instance, the laboratory results provide a test of accuracy of the numerical methods used.

The experiments reported here were primarily designed to test some aspects of a model of transient steam flow in a vapor-dominated geothermal system. The geology and hydrology of vapor-dominated systems have been extensively discussed by White, Muffler and Truesdell (1971). Typically composed of fractured rock, the reservoir has mainly fracture permeability. However, according to White, Muffler and Truesdell (1971), the unbroken rock also has small but finite porosity and permeability. These authors hypothesized that although most of the pore volume is filled with steam, there is a small residual liquid saturation in the pore space.

Moench and Atkinson (1978) developed a numerical model of steam flow in a vapor-dominated system that was loosely based on the conceptual model of White, Muffler and Truesdell (1971). For simplicity, Moench and Atkinson did

not address the dual porosity problem, but instead assumed the reservoir consisted of a uniform porous medium. They found that simulated steam-well, pressure-transient tests were drastically changed when it was assumed that a small liquid saturation was present in the reservoir. The liquid provided an extra source of steam that buffered pressure changes, and caused a large delay in pressure-transient response.

Moench and Atkinson assumed that the vapor pressure of the liquid water in the system was that of pure free water; however, the vapor pressure in an unsaturated porous medium is less that that of free water (Edelfson and Anderson, 1943). This "vapor-pressure lowering" (VPL) effect is due to the reduction of the free energy of the water in the pores. The effect becomes more pronounced at low liquid-water saturations when the water is adsorbed in a thin film on the solid surface. Viewed from a different perspective, one effect of VPL is to make adsorbed water stable in a porous medium at vapor pressures much below the saturated vapor pressure. Thus if VPL occurred in a vapor-dominated system, adsorbed water would be present even if the steam pressure was less than the saturated vapor pressure.

In Moench and Herkelrath (1978), a hypothetical VPL effect was incorporated into the model of Moench and Atkinson (1978). As expected, because some adsorbed water was assumed to be present, simulations of pressure-transient well tests showed large time lags in the pressure response, even when the steam was "superheated". However, these modeling results were necessarily considered hypothetical because the equation being used and several assumptions of the model were completely untested in the temperature and pressure regime of interest. In particular, it was unclear whether VPL would occur at high temperature. It was not known if the model correctly described transient steam flow in even the simplest homogeneous, isotropic

porous medium. The laboratory work was designed to address this question. The objective was to find out if the model could be successfullly used to simulate laboratory investigations of transient steam flow in uniform porous materials.

THEORY

The steam-flow model used was basically that developed by Moench (1976) and Moench and Atkinson (1978), which was modified to take adsorption and vapor-pressure lowering into account (Moench and Herkelrath, 1978). Steam flow in a homogeneous, isotropic porous medium was assumed to be described by Darcy's Law:

$$\vec{v} = \frac{-KK_{rv}\vec{\nabla}P_v}{\mu_v} \quad . \tag{1}$$

Variables in the equations are defined in table 1. Combining equation 1 with conservation of mass,

$$-\vec{\nabla}\cdot(\rho_v\vec{v}) = \phi\frac{\partial(\rho_v(1-S))}{\partial t} + q \tag{2}$$

yields the time-dependent steam-flow equation,

$$\vec{\nabla}\cdot\left(\frac{\rho_v KK_{rv}\vec{\nabla}P_v}{\mu_v}\right) = \phi\frac{\partial(\rho_v(1-S))}{\partial t} + q \quad . \tag{3}$$

This equation differs from the standard gas-flow equation in that a sink term for steam, q, has been added to account for adsorption of water.

A relation similar to equation 3 can be written to describe flow of liquid or adsorbed phase. However, it was assumed in the model that the adsorbed water was immobile and incompressible, so that the equation reduced to

$$q = \phi\rho_\ell\frac{\partial S}{\partial t} \tag{4}$$

The energy equation can be written as follows:

$$\vec{\nabla}\cdot(k\vec{\nabla}T) - C_1\vec{v}\cdot\vec{\nabla}T + L_v q + \frac{\phi^2(1-S)^2\mu_v v^2}{KK_{rv}} + \phi(1-S)T\beta\left(\vec{v}\cdot\vec{\nabla}P_v + \frac{\partial P_v}{\partial t}\right) = H_c\frac{\partial T}{\partial t} \tag{5}$$

The terms in equation 5 have the following physical interpretations:

$\vec{\nabla} \cdot (k\vec{\nabla}T)$	heat conduction term
$C_1\vec{v} \cdot \vec{\nabla}T$	heat convection by vapor movement.
$L_v q$	rate of release of latent heat in the steam adsorption process.
$\phi^2 \frac{(1-S)^2 \mu_v v^2}{KK_{rv}}$	rate of heat production by viscous dissipation
$\phi(1-S)T\beta(\vec{v}\cdot\vec{\nabla}P_v + \frac{\partial P_v}{\partial t})$	rate of production of heat by compressible work
$H_c \frac{\partial T}{\partial t}$	rate of change of heat storage in the porous medium

Numerical experiments were run to determine if any of the terms in the energy equation were small enough to be neglected. For the conditions of the laboratory experiments, it was found that the heat conduction and convection terms always were negligible. The viscous dissipation and compressible work terms were also generally small; however, these terms did become comparable to the latent heat and heat-storage terms when the steam-flow velocity was high. For this reason, the simplified energy equation that was used was

$$L_v q + \frac{\phi^2(1-S)^2 \mu v^2}{KK_{rv}} + \phi(1-S)T\beta(\vec{v}\cdot\vec{\nabla}P_v + \frac{\partial P_v}{\partial t}) = H_c \frac{\partial T}{\partial t} \qquad (6)$$

Another equation relating pressure and temperature was required to solve the transient steam-flow problem. Moench and Atkinson (1978) assumed that the steam pressure in a partly-saturated porous medium was equal to the saturated vapor pressure of pure water. Therefore, they assumed the steam pressure was a unique function of temperature, defined by the saturated vapor-pressure

curve. However, in order to take vapor-pressure lowering into account, the steam pressure must also be considered to be a function of the amount of water adsorption:

$$P_v = P_v(T,S) = P_o(T)R(S) \ . \tag{7}$$

$P_o(T)$ represents the saturated vapor-pressure function, and R(S) is the function relating the relative vapor pressure in the porous material to the fraction of the pore space that is filled with adsorbed water.

Moench and Atkinson developed a finite-difference method of solving the equations for one-dimensional, radially-symmetric flow to steam wells. Because radially-symmetrical flows are relatively difficult to establish in laboratory experiments, we chose instead to test the equations and the numerical procedures with one-dimensional, linear flow system. Thus the equations that were solved were the following:

(flow)
$$\frac{\partial}{\partial z}\left(\rho_v \frac{KK_{rv}}{\mu_v}\frac{\partial P_v}{\partial z}\right) - q = \phi \frac{\partial (\rho_v (1-S))}{\partial t} \tag{8}$$

(energy)
$$L_v q + \frac{\phi^2 (1-S)^2 \mu v^2}{KK_{rv}} + \phi(1-S)T\beta\left(v\frac{\partial P_v}{\partial z} + \frac{\partial P_v}{\partial t}\right) = H_c \frac{\partial T}{\partial t} \tag{9}$$

The experiments were run by flowing pure steam axially through a uniformly-packed cylinder of unconsolidated porous material. The cylinder was initially brought to a constant temperature and pressure throughout. Then the steam pressure was abruptly increased at one end (z=0), and the resulting pressure transient was measured with a pressure transducer at the other end (z=L) of the cylinder, which was closed to provide a zero-flow boundary. The

initial conditions and boundary conditions were thus the following:

$$t<0 \quad P_v=P_i, \text{ all } z$$

$$t<0 \quad T=T_i, \text{ all } z$$

$$t\geq 0 \quad P_v=P_f, \; z=0$$

$$t\geq 0 \quad \partial P_v/\partial z=0, \; z=L \text{ (no flow)}$$

Details of the solution of the equations, subject to these boundary condition, are given in the appendix.

EXPERIMENTAL METHODS

A schematic diagram of the experimental setup is given in figure 1. The system consisted of a main steam reservoir, a holder for the porous material, an auxillary steam reservoir, pressure transducers, and pneumatic valves. In order to avoid steam condensation in the lines, the entire apparatus was built inside an oven so that all components operated at the sample running temperature.

This apparatus was used in three series of experiments:

(1) Transient flow of noncondensable gases in porous media.

(2) Transient steam flow in porous media at elevated temperatures.

(3) Water adsorption and vapor-pressure lowering in porous media at elevated temperatures.

All experiments were carried out using the same sample of unconsolidated natural soil obtained at a site of Olmstead's (1977) near-surface temperature survey. Physical properties of this sandy soil are listed in Table 2. Unconsolidated material was used in order to obtain a homogeneous sample. This was accomplished through the careful packing procedure described by Ripple, James, and Rubin (1973). The fraction of the soil that passed through a 125μm sieve was densely packed into a sample holder which consisted of a stainless steel pipe 61 cm long with an internal diameter of 5.04 cm. The sample was retained in the holder by fine stainless steel screens that were fastened with epoxy cement to the stainless steel plates that formed the ends of the sample holder.

Design of the transient gas-flow experiments was based upon the classic work of Aronofsky and coworkers (Aronofsky and Jenkins, 1952; Aronofsky, 1954; Aronofsky and Ferris, 1954; Wallick and Aronofsky, 1954). These petroleum engineers obtained excellent agreement between noncondensable gas-flow theory and transient gas-flow experiments they performed using porous cores in the

laboratory. We repeated their experiments using dry nitrogen gas as a check on our experimental system.

The procedure of the nitrogen gas-flow experiments was to bring the sample to a uniform initial pressure, and then make a step increase in pressure at the top of the sample while monitoring the pressure-transient breakthrough at the bottom. The constant pressure source at the top of the sample was provided by filling the large reservoir with dry nitrogen and controlling the pressure with a regulator. The reservoir was needed as a ballast tank because the flow rate at the beginning of the experiment was large, and the pressure regulator alone could not provide enough flow. After the sample was pumped to the desired starting pressure, the pneumatic valve between the gas-filled reservoir and the sample was opened, abruptly increasing the pressure at the top of the sample. The resulting changes in pressure were monitored with pressure transducers at the top and bottom of the sample.

Transient steam-flow experiments were run in much the same manner as the gas-flow tests. The main reservoir inside the oven was filled with water to serve as a source of steam at the saturated vapor pressure of water at the system temperature. Two fine screens were placed between the reservoir and the sample in order to trap water drops entrained in the flowing steam. In preparation for a pressure-transient experiment, the system was brought to operating temperature and the sample was pumped to vacuum. In order to set the pressure to the desired initial steam pressure, the sample was exposed to an auxiliary steam source consisting of a water reservoir in a temperature bath outside the oven. The temperature of the auxiliary bath was adjusted to provide steam at the desired initial pressure. Once the steam pressure inside the sample had reached equilibrium, the valve to the auxiliary reservoir was

shut. Just as in the gas-flow experiment, a step increase in pressure was then imposed at the top of the sample by rapidly opening the pneumatic valve between the sample and the main steam reservoir. The breakthrough of steam pressure was then observed with the pressure transducers above and below the sample.

Because it was found that adsorption of water played an important role in controlling steam transport, the apparatus was also used to obtain water adsorption isotherms at elevated temperature. For this application, the sample was brought to the temperature of interest, evacuated, and then exposed to the auxiliary bath steam source for 24 hours. Because the auxiliary bath temperature was lower than the sample temperature, the resulting steam pressure in the sample was less than the saturated vapor pressure of water at the sample temperature. Despite this condition, a large amount of water was adsorbed in the sample. After equilibration, the amount of adsorption was measured by closing the sample isolation valves, letting the sample cool, and weighing it. By repeating this procedure at many different auxiliary bath temperatures, the dependence of the amount of adsorption upon relative vapor pressure was determined.

RESULTS

Transient nitrogen flow tests were run first as a check on the measurement system. Experiments were run with a variety of initial pressures ranging from 0.1 to 1.0 bar, and a final pressure of 1.0 or 2.0 bars. The results are summarized in figure 2, which is a plot of pressure at the bottom of the sample as a function of the time since the step increase in pressure occurred at the top. As shown in the figure, pressure equilibrium occurred in 15 seconds or less.

A simplified version of the computer program described in the appendix was used to simulate the experiments. To describe one-dimensional nitrogen flow, equation 8 was reduced to the standard noncondensable gas flow equation:

$$\frac{\partial}{\partial z}\left(\frac{\rho_n K}{\mu_n}\frac{\partial P_n}{\partial z}\right) = \phi\frac{\partial \rho_n}{\partial t} \tag{10}$$

It was found in the analysis that inclusion of Klinkenberg slip effect (Klinkenberg, 1941) significantly changed the simulated pressure-transient response. The slip effect is illustrated in figure 3, which is a plot of the measured permeability to nitrogen gas versus the inverse mean pressure in the sample. These data were obtained by establishing steady-state nitrogen flow in the porous medium and measuring the pressure drop across the sample, ΔP_n, and the volume flow rate, v. The permeability was determined from the relation

$$K = \frac{-\mu_v v L}{\Delta P_n} \tag{11}$$

This was repeated at many different mean pressures in order to obtain the curve of figure 3. As the graph shows, the permeability increases as a linear function of the inverse of the mean pressure, $\bar{P}_n$:

$$K = K_o(1 + b/\bar{P}_n) \tag{12}$$

The result of including the Klinkenberg effect in the theoretical analysis is illustrated in figure 4. When K is assumed to be a function of $\bar{P}$ as in equation 12, the pressure-transient response is significantly faster.

Plots of the computer simulation of the nitrogen experiments are given in figure 2 for comparison with the data. The Klinkenberg effect was incorporated into the theory through equation 12. The agreement between theory and experiment is generally good. Apparently the standard gas-flow theory provides an adequate description of the transient nitrogen-flow experiments.

Transient steam-flow experiments were run on the same sample that was used in the nitrogen-flow tests. Experiments were run with initial sample temperatures of 100°, 125°, and 146°C, and initial sample pressures ranging from 0.2 to 0.8 bar. The final pressure, which was approximately equal to the saturated vapor pressure of the water in the reservoir, ranged from 1.0 to 4.0 bars. The results are shown in figure 5, which is a plot of the steam pressure at the bottom of the sample as a function of the time since the step increase in pressure was applied at the top. As shown in figure 5, comparison of the results with the standard gas-flow theory indicated that the time required for the steam pressure to equilibrate in the experiments was 10 to 25 times greater than for noncondensable gas.

At least two pressure-transient runs were made at each temperature and initial pressure. Agreement between replicate experiments was quite good; pressure measurements taken at the same time intervals in separate experiments agreed with one another to within 5 percent of the mean reading. There was no measurable change in the system response time or in the sample permeability, despite exposure to high-temperature steam for many days. This was verified through transient nitrogen-flow tests run before and after the steam-flow

experiments. The nitrogen flow characteristics were unchanged by months of temperature and pressure cycling.

We assumed that the delay in the steam pressure response was caused by adsorption of steam in the sample. In order to test this hypothesis, the experiments were simulated using the modified steam-flow theory.

The analysis required the determination of the R(S) function defined in equation 7. In order to simplify the calculations, we assumed that the amount of adsorption at a given relative vapor pressure was given by the experimentally determined equilibrium water adsorption isotherm. This amounts to neglecting the kinetics of the adsorption process, and assuming that equilibrium between the phases was obtained instantly.

A complete adsorption isotherm was determined experimentally at 100°C. Because of equipment failure, however, only a few points on the 125° and 146°C isotherms were measured. All the adsorption data are shown in figure 6, a plot of the relative vapor pressure in the sample versus the fraction of the pore space that was filled with adsorbed water. Similar data were reported by Hsieh (1980), who determined water-adsorption isotherms for sandstone and unconsolidated sand at temperatures up to 190°C.

The adsorption was expressed in terms of liquid saturation in order to fit into the structure of the model. However, in the experiments, it was the mass rather than the volume of the adsorbed water that was measured. In order to convert the mass to liquid saturation we assumed that the adsorbed water had the same density as pure water at the prevailing temperature. This assumption is not crucial; the simulations of the pressure-transient experiments are not sensitive to changes in the assumed density of the adsorbed water.

To simplify the numerical calculations, the R(S) function was obtained by least-square fitting the 100°C adsorption data to the empirical relation

$$R(S) = 10^{-10^{(A-S)/B}} \tag{13}$$

The 100°C curve was used for all the simulations because the adsorption data at higher temperature were incomplete. This was a source of error in the calculations because the adsorption isotherm shifted slightly at higher temperatures. However, the simulations were influenced only by changes in the slope of the adsorption isotherm, and the data indicated that the slope was not highly temperature dependent.

Results of the steam-flow simulations are compared to the experimental data in figure 7. Parameters used in the calculations are given in table 3. As shown in the graphs, the comparison between theory and experiment is excellent for all the runs, thus supporting the assumptions of the model for the conditions of the study.

In simulating steam pressure-transient behavior, the computer program generated theoretical depth profiles of pressure, temperature, and liquid saturation during the experiments. The predicted distribution of these variables for the 100°C experiment is shown in figures 8, 9, and 10. The experimental apparatus does not presently permit the measurement of these variables within the sample. However, study of the theoretical profiles aids in understanding the dynamics of the system. As indicated in the graphs, we assumed in the calculation that pressure, temperature and adsorption were initially uniform. The initial liquid saturation was found by inverting equation 13:

$$S = A - B \log_{10}\left\{\log_{10}(P_o(T_i)/P_i)\right\} \tag{14}$$

When the pressure was increased at the top of the sample (figure 8), additional adsorption occurred near the top (figure 10). When the steam was adsorbed, latent heat was released, which resulted in a temperature increase (figure 9). As time increased, fronts of increasing pressure, temperature, and amount of adsorption passed through the porous medium, eventually reaching the bottom.

DISCUSSION

The results support the hypothesis that the delay in the steam-pressure breakthrough was caused by adsorption of steam in the porous sample. The good agreement between theory and experiment shown in figure 7 is encouraging support for the modified steam-flow model. It should be emphasized that no fitting was done to obtain the theoretical curves; all the parameters were measured independently. However, the experimental tests were incomplete in that the dependence of pressure, temperature, and amount of adsorption upon depth and time were not measured. Additional terms might have to be incorporated into the theory in order to describe adequately pressure-transient behavior near the input end of the sample. For example, where the pressure gradient and the rate of increased pressure were large, the kinetics of the adsorption process might be important. The experimental apparatus should be improved to enable measurements within the sample for comparison to the simulated profiles shown in figures 8, 9, 10. Also, complete adsorption isotherms should be measured at 125°, and 146°C in order to test the model at these temperatures properly.

It is important to recognize that an extremely simplified form of the theory has been tested in the experiments. Depending upon the application, many other factors could be included in the model and tested in the experiments.

Investigation of the mechanisms of steam adsorption was beyond the scope of this work. The approach was to treat the adsorbing medium as a "black box", the properties of which were determined empirically as in figure 6. To the extent that agreement between theory and experiment was obtained the approach was adequate. However, what this means is that at present the steam

adsorption isotherm of the material must be known before reasonable predictions can be made about pressure-transient behavior.

These considerations limit the speculations that one can make about the effect of adsorption upon transient steam flow in the field. It is probable, however, that most of the steam is adsorbed in the clay fraction, where specific surface is greatest. We thus suppose that adsorption effects would be most pronounced in field areas in which the porous media contained large amounts of clay. For example, steam well tests in geothermal zones containing alteration products in the reservoir might be affected by adsorption effects (Moench and Herkelrath, 1978). On the other hand, similar tests in a "clean" part of the reservoir would not be strongly influenced, and the pressure response could be correctly interpreted without considering adsorption effects.

References

Aronofsky, J. S., 1954, Effect of gas slip on unsteady flow of gas through porous media: Journal of Applied Physics, v. 25, no. 1, p. 48-53.

Aronofsky, J. S., and Ferris, O. D., 1954, Transient flow of non-ideal gases in porous solids - one-dimensional case: Journal of Applied Physics, v. 25, no. 10, p. 1289-1293.

Aronofsky, J. S., and Jenkins, R., 1952, Unsteady flow of gas through porous media, one-dimensional case: Proceedings of the First U.S. National Conference on Applied Mechanics, American Society of Mechanical Engineers, New York, p. 763-771.

Dorsey, N. E., 1968, Properties of ordinary water-substance: New York, Hafner Publishing Co., 673 p. (Facsimile of the 1940 addition).

Edelfson, N. E., and Anderson, A. B. C., 1943, The thermodynamics of soil moisture: Hilgardia, v. 16, p. 31-299.

Hsieh, Chih-Hang, 1980, Vapor pressure lowering in porous media: Stanford University, Stanford, California, Ph. D. thesis.

Moench, A. F., 1976 Simulation of steam transport in vapor-dominated geothermal reservoirs: U.S. Geological Survey Open-File Report 76-607, 43 p.

Moench, A. F., and Atkinson, P. G., 1978, Transient-pressure analysis in geothermal steam reservoirs with an immobile vaporizing liquid phase: Geothermics, v. 7, p. 253-264.

Moench, A. F., and Herkelrath, W. N., 1978, The effect of vapor-pressure lowering upon pressure drawdown and buildup in geothermal steam wells: Transactions, Geothermal Resources Council Annual Meeting, Hilo, Hawaii, July 25-27, p. 465-468.

Olmstead, F. H., 1977, Use of temperature surveys at a depth of 1 meter in geothermal exploration in Nevada: U.S. Geological Survey Professional Paper 1044-B, 25 p.

Ripple, C. D., James, R. V., and Rubin, J., 1973, Radial particle-size segregation during packing of particles into cylindrical containers: Powder Technology, v. 8, p. 165-175.

Rosenberg, D. U., von, 1969, Methods for numerical solution of partial differential equations: New York, American Elsevier Publishing Co., Inc., 128 p.

Wallick, G. C., and Aronofsky, J. S., 1954, Effect of gas slip on unsteady flow of gas through porous media - experimental verification: Transactions of American Institute of Mechanical Engineers, Petroleum Branch, v. 201., p. 322-324.

White, D. E., Muffler, L. J. P., and Truesdell, A. H., 1971, Vapor-dominated, hydrothermal systems compared with hot-water systems: Economic Geology, v. 66, p. 75-97.

APPENDIX

Following the approach of Moench and Atkinson (1978), equations 8 and 9 were solved using a fully-implicit technique in order to avoid numerical instability. Truncation error introduced by the method was minimized by using small time and space increments. Properties of pure steam were computed from empirical relationships given by Dorsey (1968).

After expanding the right hand side of equation 8 in terms of temperature and pressure, the implicit difference form of the flow equation can be written as:

$$\Delta(T_v \Delta\delta P) + \Delta(T_v \Delta P^n) - q^n \Delta z = b_1 \phi (1-S^n) \rho_v \kappa \delta P + b_1 \phi (1-S^n) \rho_v \beta (\delta T)^n - b_1 \phi \rho_v (\delta S)^n \qquad (A1)$$

in which $b_1 = \Delta z / \Delta t$

$$T_v = \rho_v \frac{K K_{rv}}{\mu_v \Delta z}$$

$$\delta P = P^{n+1} - P^n$$

$$(\delta T)^n = T^n - T^{n-1}$$

$$(\delta S)^n = S^n - S^{n-1}$$

Time steps are integer values of n, where n+1 is the new time step. Problems of instability due to nonlinearities were avoided by using very small time steps. The parameters κ and β are the steam isothermal compressibility and thermal expansivity, respectively. Equation A1 was written in terms of pressure and temperature changes, δP and δT, rather than in absolute values in order to reduce roundoff error.

The finite-difference operators in Equation A1 can be written as:

$$\Delta(T_v \Delta\delta P) = T_{v,i+\frac{1}{2}} (\delta P_{i+1} - \delta P_i) - T_{v,i-\frac{1}{2}}(\delta P_i - \delta P_{i-1})$$

and $$\Delta(T_v \Delta P^n) = T_{v,i+\frac{1}{2}} (P^n_{i+1} - P^n_i) - T_{v,i-\frac{1}{2}} (P^n_i - P^n_{i-1})$$

where i = node number.

Substituting this operator into equation A1 and rearranging, with all known terms on the right hand side, the following expression is obtained.

$$A_i \, \delta P_{i-1} + B_i \, \delta P_i + C_i \, \delta P_{i+1} = D_i \qquad \text{(A2)}$$

where $A_i = T_{v,i-\frac{1}{2}}$,

$B_i = -(T_{v,i+\frac{1}{2}} + T_{v,i-\frac{1}{2}} + b_1\phi(1-S)\rho_v\kappa)$,

$C_i = T_{v,i+\frac{1}{2}}$,

and $D_i = -T_{v,i+\frac{1}{2}}(P^n_{i+1} - P^n_i) + T_{v,i-\frac{1}{2}}(P^n_i - P^n_{i-1})$

$+ q^n_i \Delta z + b_1\phi(1-S^n)\rho_v\beta(\delta T)^n - b_1\phi\rho_v(\delta S)^n$

The transmissive parameters are approximated as:

$$T_{v,i+\frac{1}{2}} \approx \tfrac{1}{2}(T_{v,i} + T_{v,i+1})$$

$$T_{v,i-\frac{1}{2}} \approx \tfrac{1}{2}(T_{v,i-1} + T_{v,i})$$

At the boundary i=1 (sample bottom) a no-flow condition was assumed, whereupon $T_{v,\frac{1}{2}}=0$. At the boundary i=m (sample top) constant pressure was obtained by defining the coefficients $A_m=C_m=D_m=0$ and $B_m \neq 0$.

The energy equation, expressed by equation 9, is in a form which permits direct calculation of temperature changes from parameters which had been evaluated at the previous time level. Temperature changes were thus calculated as follows:

$$\delta T_i = (a_1 + a_2 + a_3)\Delta t/H_c \qquad \text{(A3)}$$

where $a_1 = L_v q_i^n$,

$$a_2 = \frac{\phi^2 (1-S^n)^2 \mu_v (v_i^n)^2}{KK_{rv}} \quad ,$$

and $$a_3 = \phi(1-S^n)T^n\beta \left[\frac{v_i^n}{\Delta z}(P_i^n - P_{i-1}^n) + \frac{(\delta P)^n}{\Delta t}\right]$$

Here v_i^n is the interstitial velocity, defined as,

$$v_i^n = -\frac{KK_{rv}}{\mu_v \Delta z \phi}(P_i^n - P_{i-1}^n) \qquad \text{(A4)}$$

The energy and flow equations were solved sequentially within a time step beginning with the explicit calculation of the temperature in equation A3 using values of parameters obtained in the previous time step. This was followed by an updating of the temperature dependent parameters including the equilibrium vapor-pressure relationship given by equation 7. Equation A2 was solved iteratively using the Thomas algorithm (Rosenberg, 1969) adjusting the sink (or rate of adsorption) term until the equation was balanced. The criterion used to establish convergence was that computed pressure be within a prescribed tolerance of the vapor-pressure defined by equation 7.

The following expression for the sink term was used in this procedure:

$$q^k = \frac{\phi(1-S)}{\Delta t}\left[\rho_v^* - \rho_v^{k-1}\right] + q^{k-1} \qquad (A5)$$

where k = iteration number

ρ_v^* = vapor density defined by equation 7.

Having computed the sink-term distribution, the change in saturation at each point was obtained directly from equation 4. Finally, velocities were obtained from equation A4 and computations proceeded to the next step.

Table 1

Notation

A and B	= fitting factors in relative vapor-pressure function
b	= Klinkenberg slip factor
C_l	= heat capacity of steam
H_c	= heat capacity of porous medium
k	= thermal conductivity
K	= permeability
K_o	= intrinsic permeability
K_{rv}	= relative permeability to steam
L	= sample length
L_v	= latent heat of vaporization
P_i	= initial steam pressure
P_F	= final steam pressure
P_n	= nitrogen pressure
P_v	= steam pressure
$P_o(T)$	= saturated vapor-pressure function
Q	= rate of heat loss by conduction
q	= rate of steam adsorption
R(S)	= relative vapor-pressure function
S	= liquid saturation, fractional
T	= temperature
T_i	= initial temperature
t	= time
v	= volume flow rate, per unit area
z	= position in sample
β	= thermal expansivity of water vapor
κ	= isothermal compressiblity of water vapor
μ_n	= viscosity of nitrogen
μ_v	= viscosity of steam
ρ_n	= nitrogen density
ρ_ℓ	= liquid water density
ρ_v	= steam density
ϕ	= porosity

Table 2

Physical Properties of Porous Medium

Particle-size (< 125 μm) distribution in weight percent:	
Sand (50μ<D<125μ)	67
Silt (2μ<D<50μ)	26
Clay (<2μ)	7
Solid density:	2.72 g/cm^3
Bulk density:	1.58 g/cm^3
Porosity:	0.42 cm^3/cm^3
Intrinsic permeability:	3.57 x 10^{-8} cm^2
Specific surface area (determined by nitrogen adsorption)	40 cm^2/g

Table 3

Values of Parameters*

A	$= 8.65 \times 10^{-3}$
B	$= 2.30 \times 10^{-2}$
b	$= 1.4 \times 10^{5}$ dynes/cm^2
H_c	$= 1.3 \times 10^{7}$ dynes/cm^2.^{o}C
K_o	$= 3.6 \times 10^{-8}$ cm^2
K_{rv}	$= 1.0$
L	$= 61.0$ cm
ϕ	$= 0.42$ cm^3/cm^3

*Remaining parameters are known properties of liquid water or steam at prevailing temperature and pressure

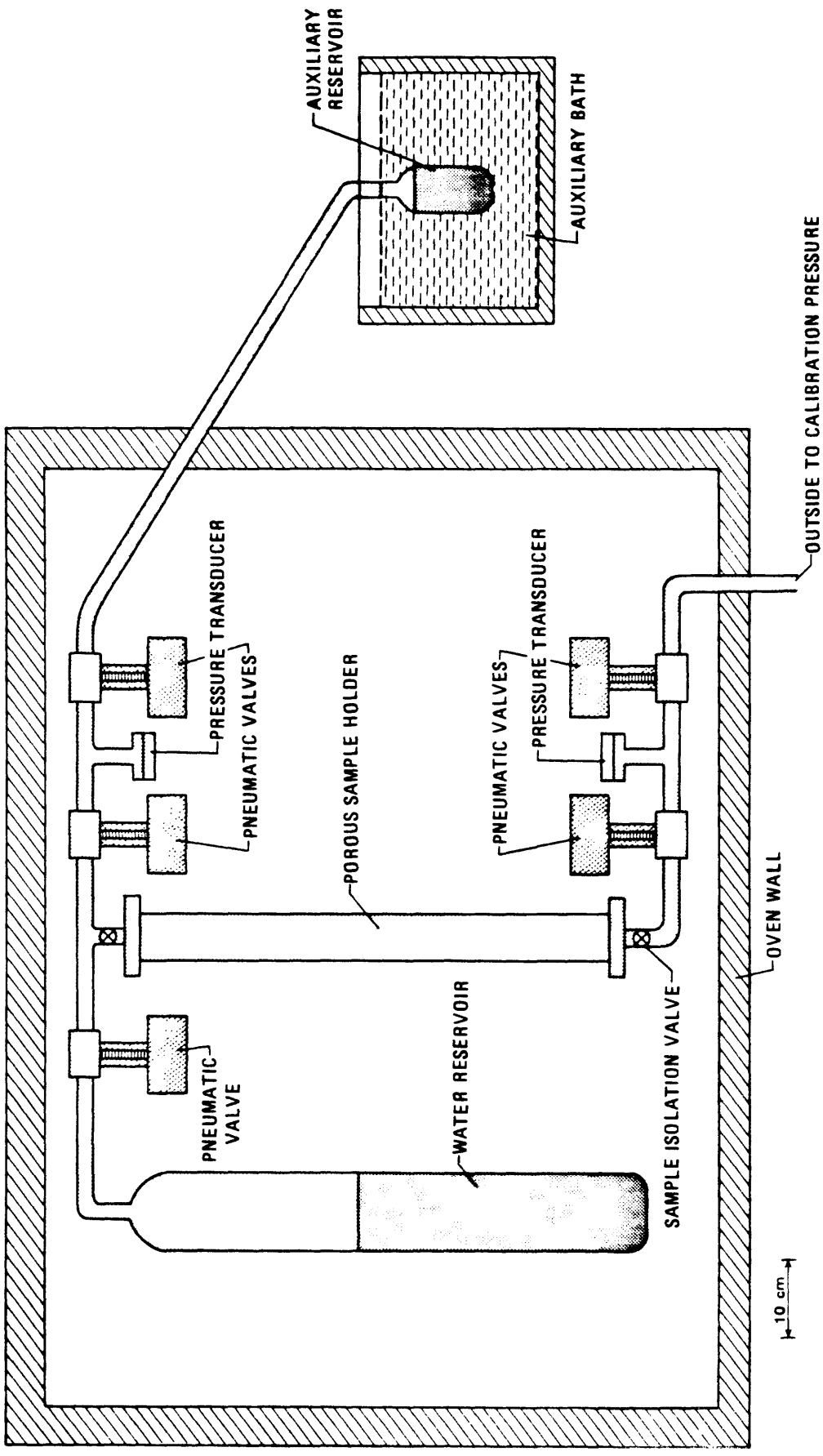

Figure 1. SCHEMATIC DIAGRAM OF STREAM-PRESSURE-TRANSIENT APPARATUS

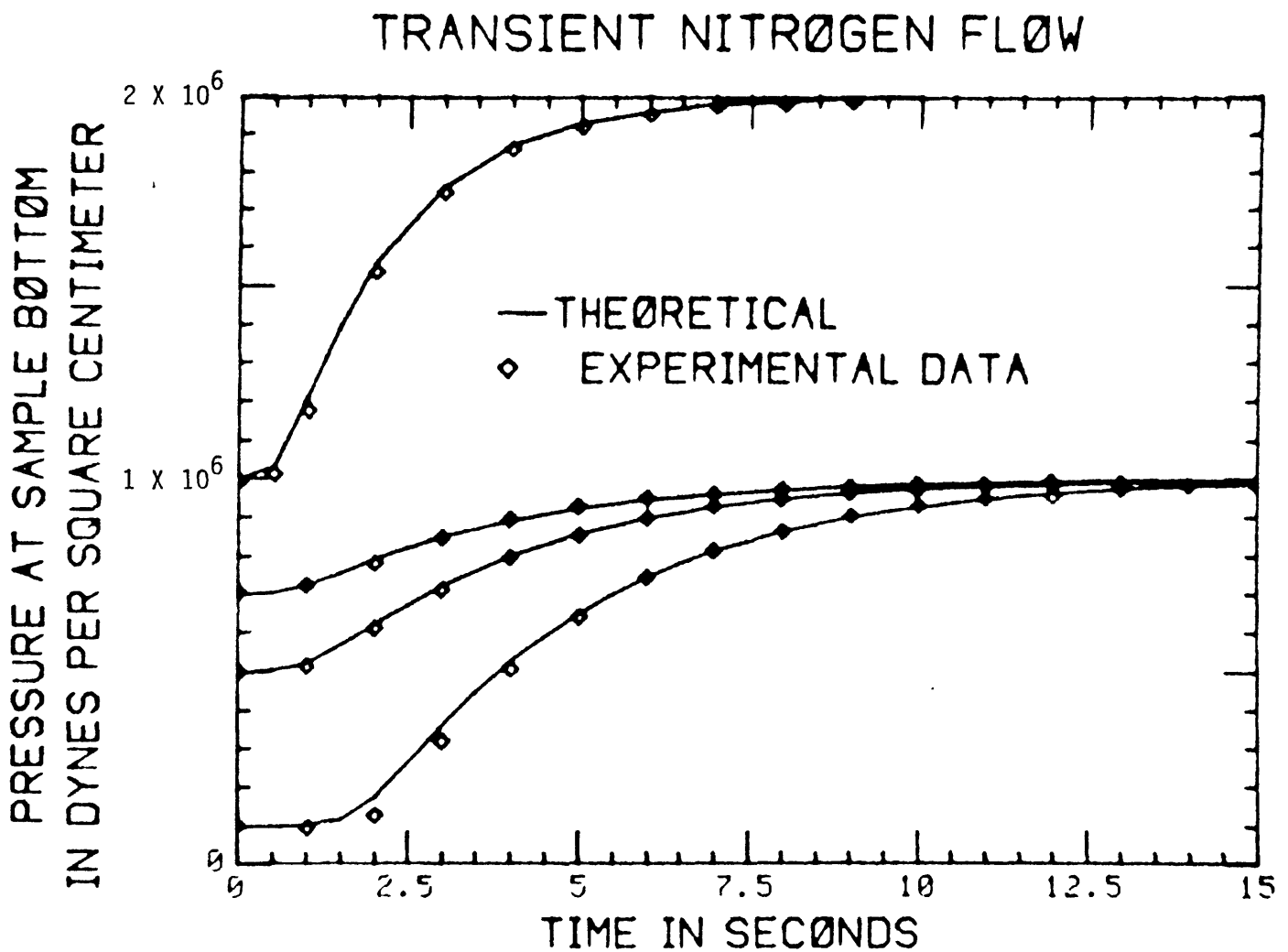

Figure 2. Nitrogen gas pressure at the closed, bottom end of the porous cylinder plotted as a function of time since a step increase in pressure was imposed at the top. The solid lines represent simulation of the experiments using standard gas-flow theory.

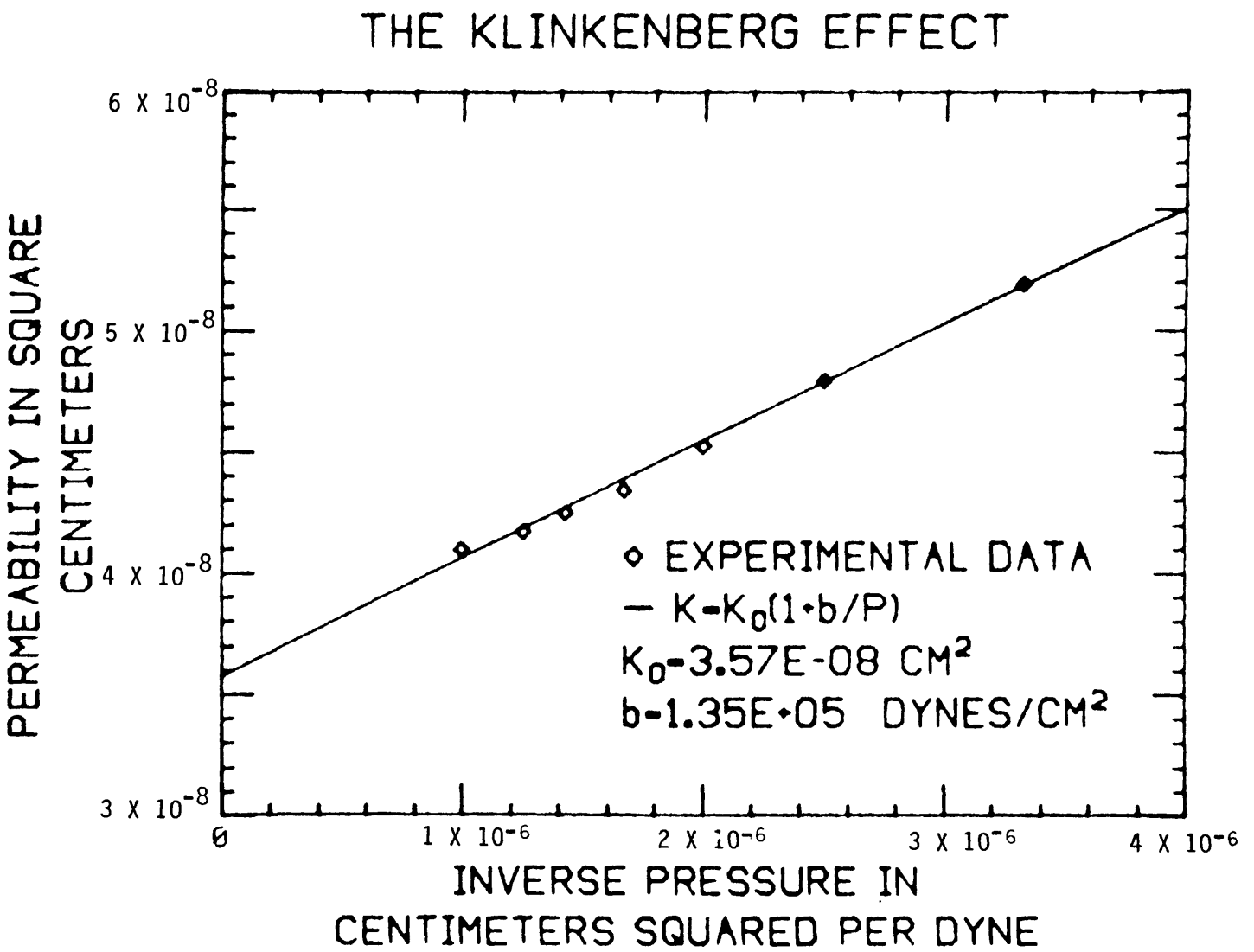

Figure 3. Measured permeability of the porous material to nitrogen gas plotted as a function of the inverse of the mean gas pressure. The straight line is the linear regression used to obtain the intrinsic permeability, K_o, and the Klinkenberg factor, b.

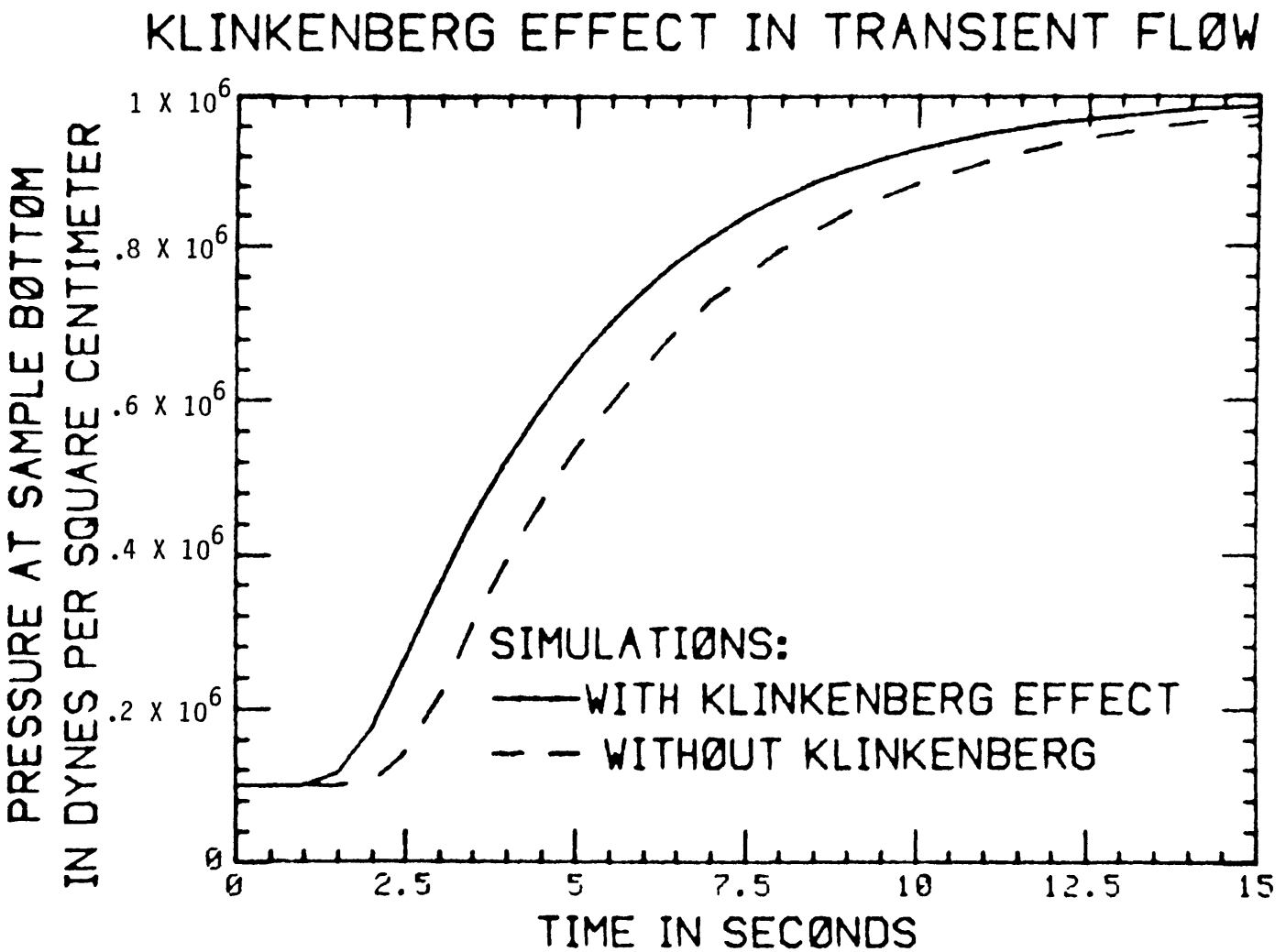

Figure 4. Demonstration of the influence of the Klinkenberg effect upon transient flow of nitrogen gas in the porous medium. The curves represent simulations of experiments with and without inclusion of the Klinkenberg effect in the gas-flow theory.

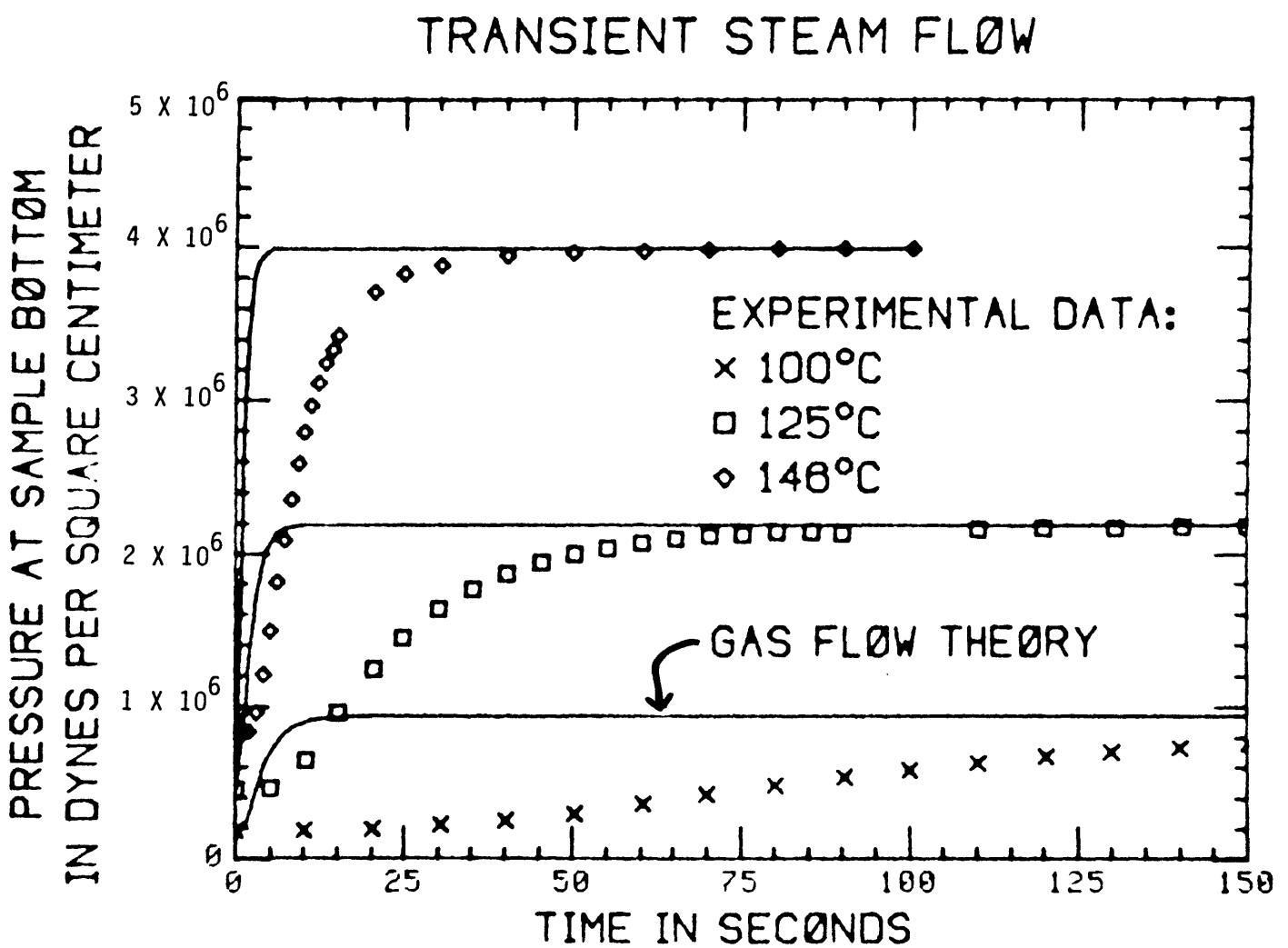

Figure 5. Steam pressure at the closed, bottom end of the porous cylinder plotted as a function of time since a step increase in pressure was imposed at the top. The solid lines represent simulation of the experiments using standard gas-flow theory.

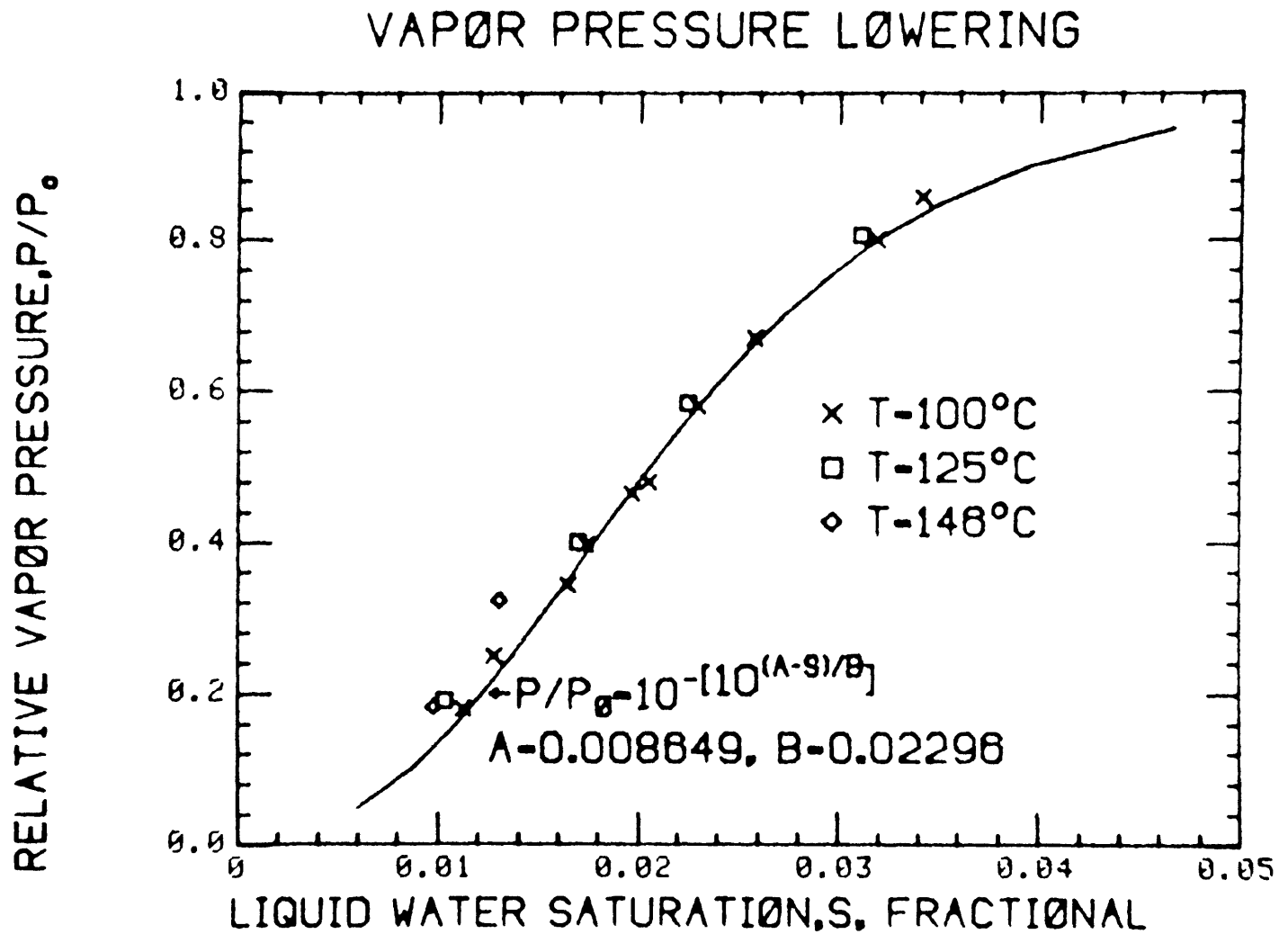

Figure 6. Equilibrium relative vapor pressure in the porous sample plotted as a function of the amount of water adsorption, expressed as liquid saturation. The solid line represents the empirical equation which was used in the steam-flow simulations.

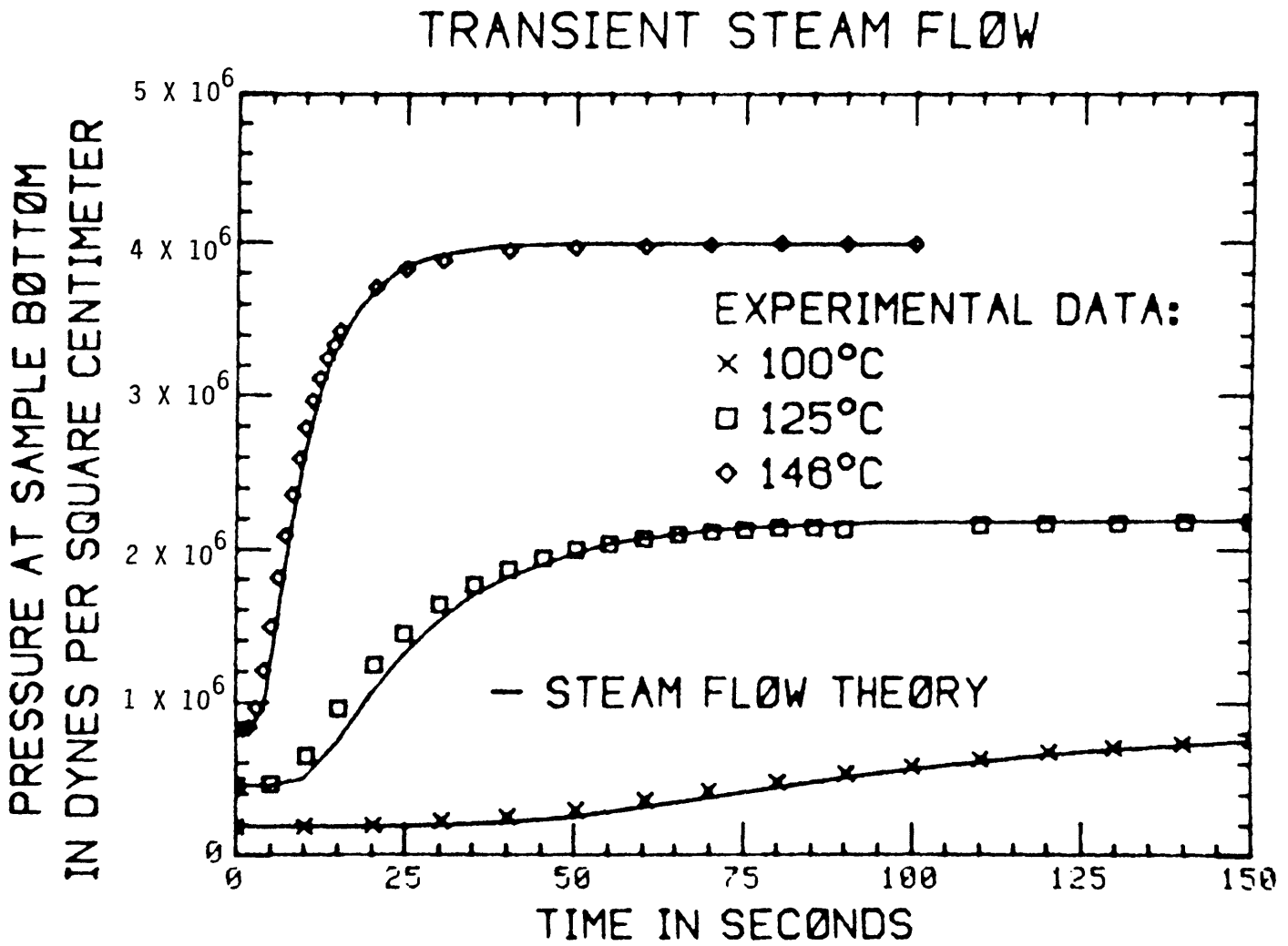

Figure 7. Steam pressure at the closed, bottom end of the porous cylinder plotted as a function of time since a step increase in pressure was imposed at the top. The solid lines represent computer simulations of the experiments using the steam-flow theory which includes a steam adsorption sink term.

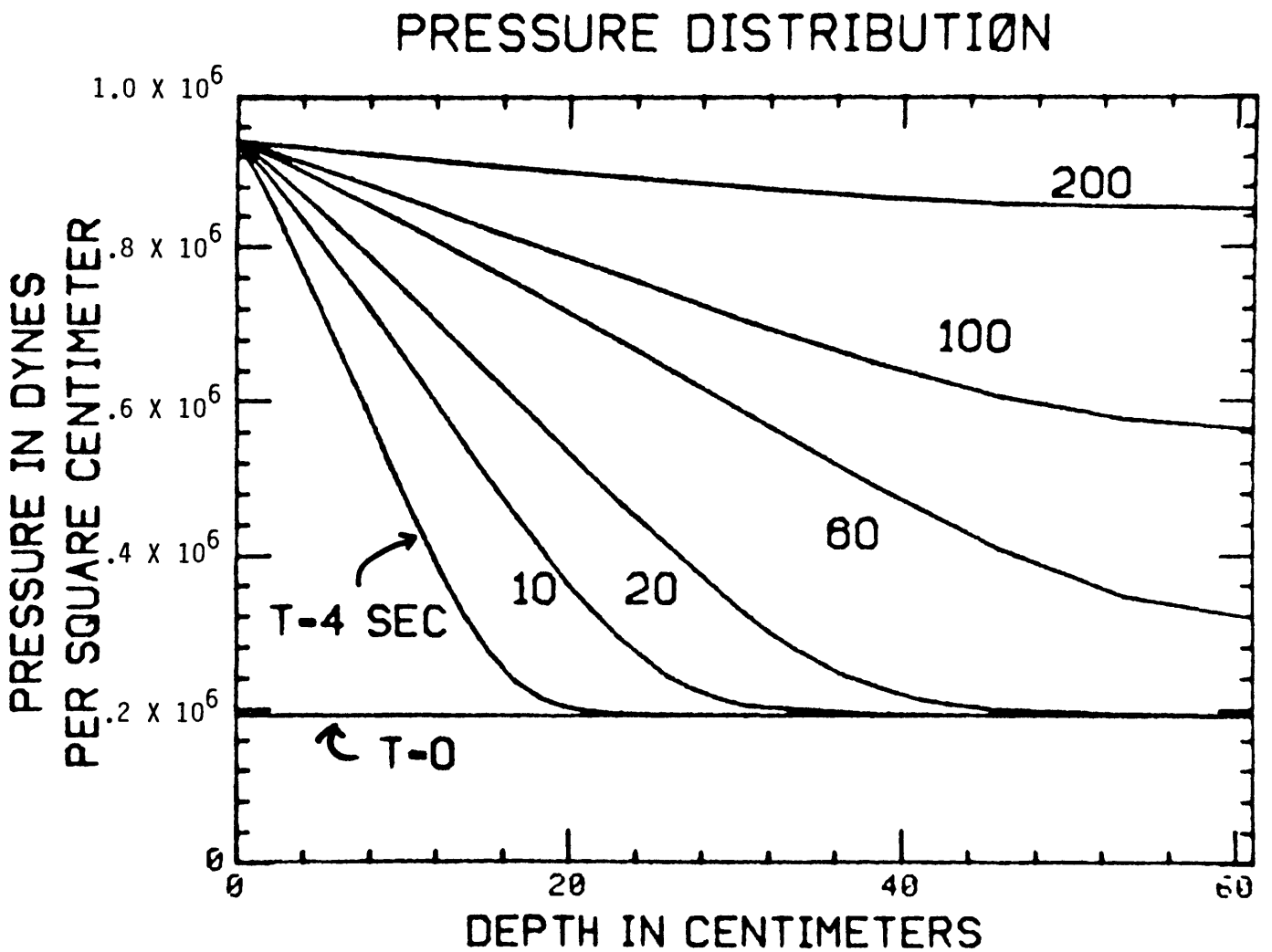

Figure 8. Simulated pressure distribution in the porous sample during the pressure-transient experiment which was run at 100°C. Numbers next to the curves indicate the time in seconds since the step increase in pressure was imposed at the top of the sample.

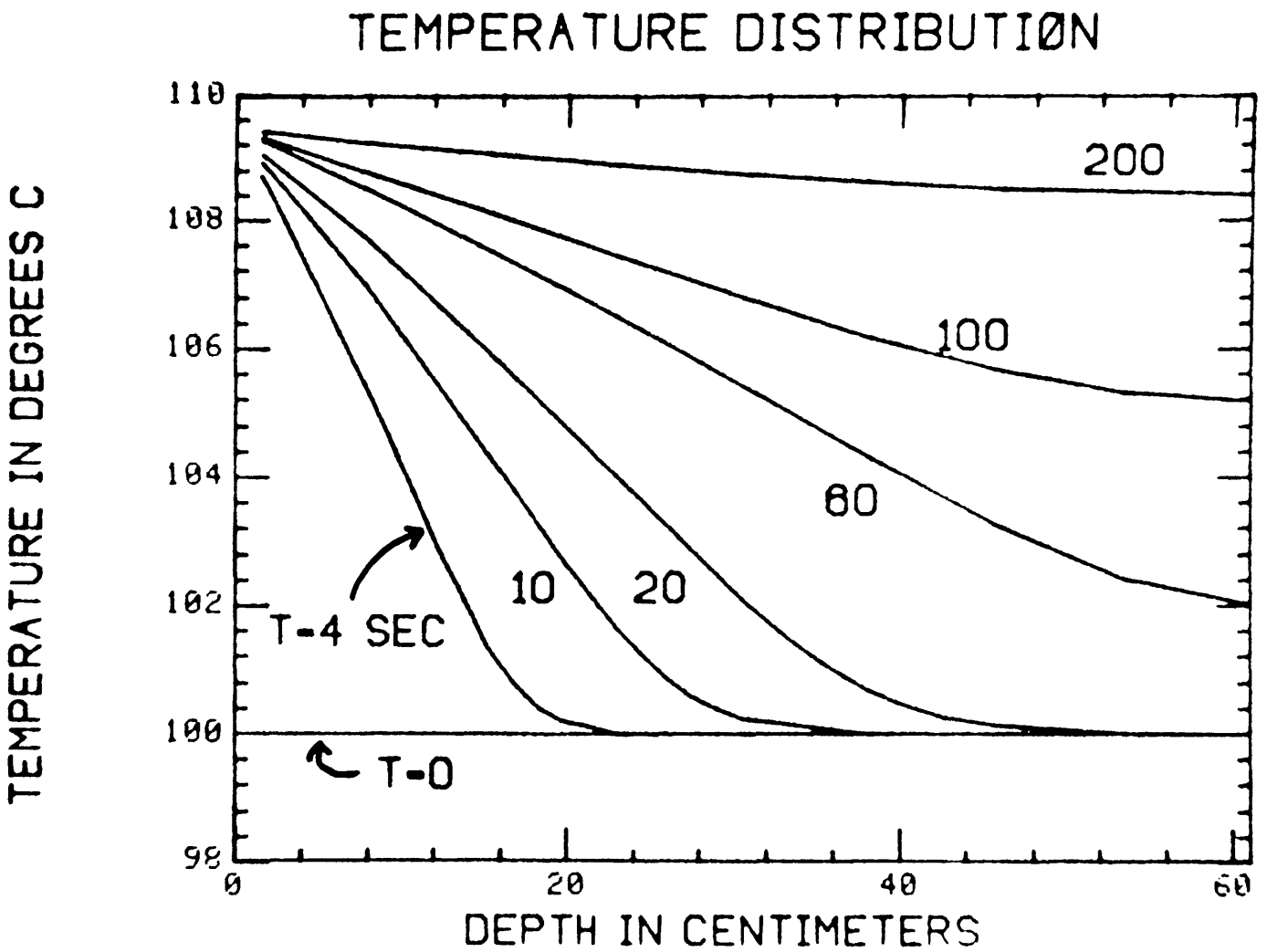

Figure 9. Simulated temperature distribution in the porous sample during the pressure-transient experiment which was run with an initial temperature of 100°C. Numbers next to the curves indicate the time in seconds since the step increase in pressure was imposed at the top of the sample.

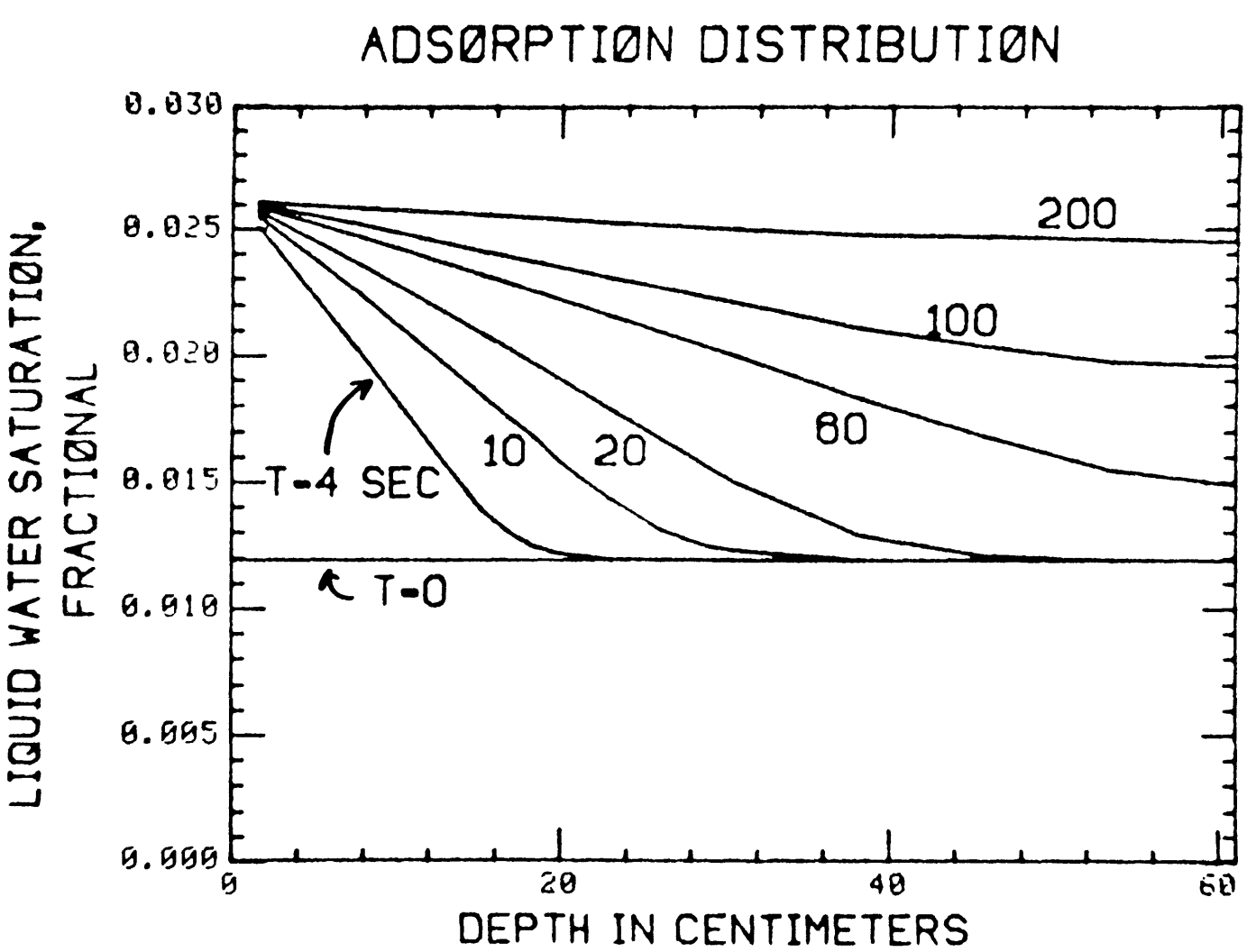

Figure 10. Simulated distribution of amount of adsorption in the porous sample during the 100°C steam pressure-transient experiment. Numbers next to the curves indicate the time in seconds since the step increase in pressure was imposed at the top of the sample.